Additional Precursor Purification in Isobaric Mass Tagging Experiments by Traveling Wave Ion Mobility Separation (TWIMS)

ARTICLE *in* JOURNAL OF PROTEOME RESEARCH · MAY 2014

Impact Factor: 4.25 · DOI: 10.1021/pr500220g · Source: PubMed

8 AUTHORS, INCLUDING:

Rebekah Jukes-Jones
Medical Research Council (UK)
21 PUBLICATIONS **711** CITATIONS
SEE PROFILE

James Langridge
Waters Corporation
101 PUBLICATIONS **2,301** CITATIONS
SEE PROFILE

Kathryn Lilley
University of Cambridge
217 PUBLICATIONS **9,759** CITATIONS
SEE PROFILE

Journal of proteome research

Article

pubs.acs.org/jpr

Additional Precursor Purification in Isobaric Mass Tagging Experiments by Traveling Wave Ion Mobility Separation (TWIMS)

Pavel V. Shliaha,[†] Rebekah Jukes-Jones,[‡] Andy Christoforou,[†] Jonathan Fox,[§] Chris Hughes,[§] James Langridge,[§] Kelvin Cain,[‡] and Kathryn S. Lilley*,[†]

[†]Cambridge Centre for Proteomics, Department of Biochemistry, University of Cambridge, Cambridge, U.K.

[‡]MRC Toxicology Unit, University of Leicester, Leicester, U.K.

[§]Waters Corporation, HRMS, Stamford Avenue, Altrincham Road, Wilmslow, SK9 4AX, U.K.

Supporting Information

ABSTRACT: Despite the increasing popularity of data-independent acquisition workflows, data-dependent acquisition (DDA) is still the prevalent method of LC−MS-based proteomics. DDA is the basis of isobaric mass tagging technique, a powerful MS2 quantification strategy that allows coanalysis of up to 10 proteomics samples. A well-documented limitation of DDA, however, is precursor coselection, whereby a target peptide is coisolated with other ions for fragmentation. Here, we investigated if additional peptide purification by traveling wave ion mobility separation (TWIMS) can reduce precursor contamination using a mixture of *Saccharomyces cerevisiae* and HeLa proteomes. In accordance with previous reports on FAIMS-Orbitrap instruments, we find that TWIMS provides a remarkable improvement (on average 2.85 times) in the signal-to-noise ratio for sequence ions. We also report that TWIMS reduces reporter ions contamination by around one-third (to 14−15% contamination) and even further (to 6−9%) when combined with a narrowed quadrupole isolation window. We discuss challenges associated with applying TWIMS purification to isobaric mass tagging experiments, including correlation between ion m/z and drift time, which means that coselected peptides are expected to have similar mobility. We also demonstrate that labeling results in peptides having more uniform m/z and drift time distributions than observed for unlabeled peptides. Data are available via ProteomeXchange with identifier PXD001047.

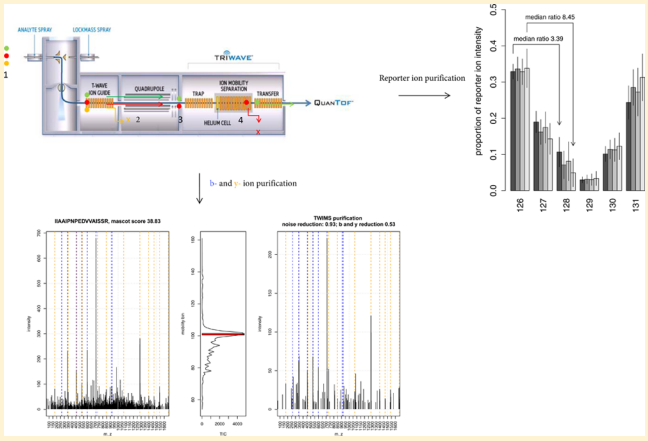

KEYWORDS: *ion mobility separation, TWIMS, isobaric tagging, tandem mass tags*

INTRODUCTION

With mass spectrometer systems becoming ever faster and more sensitive, routine LC−MS analysis has come even closer to identifying almost all of the proteins in a given sample.[1−3] Thus, instrument and method development has focused on improving multiplexing sample analysis to save instrument time by quantitatively analyzing as many samples as possible during one LC−MS acquisition.

A number of approaches have been developed to relatively quantify two or three samples within one LC−MS acquisition: including ^{18}O,[4] conventional SILAC,[5,6] ^{15}N[7] and *N*−*N*-dimethyl labeling.[8] Two techniques have been described that could potentially analyze significantly more than two samples together: isobaric mass tagging[9] and neutron encoded mass signature SILAC.[10] The latter is an MS1 multiplexing technique which requires extremely high resolution MS, currently available on high-field Orbitrap models and FT-ICR instruments only. Also, as with conventional SILAC, this technique requires *in vivo* labeling, which is not feasible for some samples.[11] Isobaric mass tagging (available commercially as iTRAQ and TMT reagents) on the other hand can be applied to any group of samples, and the resolution necessary for accurate quantification can easily be obtained on most commercial TOF and Orbitrap instruments. Isobaric tagging involves labeling a sample with one of up to 10 different tags of isobaric mass. During fragmentation in MS2, a tag yields a low mass reporter ion specific to the tag. In this way samples labeled with different isobaric tags can be combined before LC−MS/MS. A peptide ion present in all samples will appear as a single ion in MS1, but in MS2 the relative intensity of the reporter ions liberated upon fragmentation represents the abundance of the peptide within the samples being compared.

An established problem associated with all DDA experiments and with isobaric mass tagging quantification in particular is precursor coselection, whereby the combined resolution of LC

Received: March 5, 2014
Published: May 22, 2014

dx.doi.org/10.1021/pr500220g | *J. Proteome Res.* 2014, 13, 3360−3369

and quadrupole *m/z* filtering is not enough to isolate pure precursors.[12,13] Instead, a number of precursors representing both peptides and chemical noise are coisolated and cofragmented. Precursor contamination results in both a decrease in peptide identification rate and decreased quantitative accuracy. A number of publications have investigated both of these effects.

Luethy et al. have estimated that in complex mixtures at least 50% of precursors are coselected for fragmentation with other peptides.[14] To evaluate coselection more quantitatively Houel et al. have developed ChimeraCounter software. At a 0.2 threshold for chimericity (defined as ratio of the intensity of the highest contaminating peak to target peak intensity), around half of MS2 spectra in proteome from K562 human cell line were classified as chimeric.[15] The chimeric spectra were less likely to be identified during database search, especially if the precursor targeted for fragmentation had low intensity. Michalski et al. have reported that the median proportion of target ion current within a typical quadrupole transmission window (4Tn) is only 14%, meaning that many of the low abundant peptides are impossible to identify by DDA workflows with currently used quadrupole mass filters.[16] In addition to precursor contamination attributable to other peptides, the identification rate is also hindered by cofragmenting singly charged ions representing solvent impurities, residual reagents used in sample preparation, substances originating from the ion source and LC system, etc. As a result, application of precursor intensity thresholding is recommended for most DDA workflows.[17,18] Fragmenting peptides with intensity below the defined threshold is highly unlikely to result in identification, due to the low S/N ratio of the resulting MS/MS spectrum.

The quantitative accuracy in isobaric mass tagging experiments is impaired by precursor coselection, since reporter ions recorded and used for quantification do not originate exclusively from the peptide of interest, but rather from all coselected peptides[19−23] (see refs 24 or 25 for review). An additional complication is that reporter ion distortion is thought to arise from coselection of a population of contaminants, each of which may individually fall below the respective limits of detection in MS1 and MS2 spectra, but collectively yield reporter ions in sufficient abundances to generate a pronounced distorting effect on relative reporter ion intensities.[25,26] As a result, it was demonstrated that precursor purity measured in MS1 is a poor predictor of quantitative accuracy in isobaric mass tagging experiments on orbitrap instruments.[21]

A clear illustration of the coselection problem comes from spiking unlabeled peptides into a complex sample labeled with the isobaric mass tags. Notably, around 70% of unlabeled peptides have all reporters present in their MS2 spectra.[25]

To investigate precursor coisolation more quantitatively, Ow et al. prepared a spike-in standard, whereby they labeled different amounts of protein standard with iTRAQ 8-plex reagent. Then four reporter channels were spiked with a *Nostoc punctiforme* complex sample, while four other contained only standard proteins which remained free from contamination.[27] This allowed prediction of the theoretically expected ratios of standard protein and their comparison with those observed experimentally.

A number of approaches have been suggested to address the problem of reporter ion contamination. Several groups have reported bioinformatics approaches to model variability of reporter ratios in individual spectra or on the protein level, based on reporter intensities, number of peptides fragmented per protein, and biological variability in samples investigated.[21,28−30] Though useful in eliminating some variability originating from low reporter intensities, these models cannot be expected to completely restore true reporter ratios especially in samples where background is not expected to be equimolar.[25]

Recently, Ting et al. took advantage of the lower collision energy required to fragment the peptide backbone compared to the TMT reporter group to improve the accuracy and precision of quantification. They introduced an approach whereby a peptide is first fragmented at low collision energy in an ion trap to produce a b- and y- ion series, and then a fragment ion is isolated and refragmented by higher energy collisional dissociation (HCD).[26] While this approach successfully restored the quantitative performance of isobaric tagging, it initially suffered from impaired sensitivity due to only a single MS2 ion being selected for MS3 fragmentation.[31] Application of attenuated ion selection waveforms in order to accumulate multiple MS2 fragments for MS3 fragmentation and coanalysis has reportedly addressed this issue.[32] A refined version of this strategy, termed "synchronous precursor selection", is available as a default data acquisition method on the Orbitrap Fusion.

A different approach termed gas-phase purification was introduced by Wenger et al., whereby the charge states of coselected precursors are reduced by proton transfer reaction, and then the charge reduced target precursor is reselected for fragmentation.[33] This effectively removes contaminants with different charge states and reduces interference from contaminants of the same charge state by expanding the *m/z* space they occupy. This resulted in 20% reduction of precursor contamination, although it did not remove contamination entirely.

Perhaps the most intuitive approach to interference reduction is extensive sample fractionation,[20] and/or targeting peptides for fragmentation at their chromatographic apexes,[34] which increases the ratio of target precursors to contaminants during fragmentation. This has been traditionally accomplished by incorporation of multidimensional chromatography in the LC−MS workflow.[26,35] There are however alternative fractionation technologies to liquid chromatography. Recently, a number of ion mobility separation (IMS-MS) platforms have been launched by major MS vendors.[36] IMS is a group of techniques that fractionates ions based on the velocity of movement through buffer gas in an electric field.[37] Importantly, ion mobility separation occurs within the hybrid IMS-MS platform and does not require an increase in instrument time. In this study we have investigated the degree to which traveling wave ion mobility separation (TWIMS) further purifies target precursors after quadrupole mass filtering in an LC−MS experiment on a Synapt G2S and Synapt G2Si platforms.[38] We have characterized the effects of TWIMS on the quantitative performance of tandem mass tags (TMT) and on purity of MS/MS spectra. As initially suggested by Evans et al., IMS could potentially decrease coselection in isobaric mass tagging experiments, provided contaminant ions have a significantly different mobilities than the target ion.[24] Two IMS properties must however be taken into consideration. First, IMS of current commercial IMS-MS hybrid instruments typically has a low resolving power (around 45 for TWIMS on the Synapt G2S) compared to state-of-the art mass analysers. Second, the mobility of an ion has been shown to correlate with its *m/z*

dx.doi.org/10.1021/pr500220g | J. Proteome Res. 2014, 13, 3360−3369

Table 1. Preparation of TMT Standard[a]

	126	127	128	129	130	131
S. cerevisiae	50 (25)	20 (10)	5 (2.5)	5 (2.5)	20 (10)	20 (50)
HeLa	50 (25)	50 (25)	50 (25)			

[a]The numbers indicate the volume of 1 μg/μL peptide solution. The numbers in parentheses indicate the volume of TMT reagent (50 μL of acetonitrile per tube used).

quite tightly for ions in the same charge state.[39] Thus, the combined peak capacity of quadrupole and IMS methods is not a product of their individual peak capacities.[40]

MATERIALS AND METHODS

Sample Preparation

The sample used in this study was prepared as described by Ting et al.[26] (Table 1).

Saccharomyces cerevisiae strain YDL227C (ΔHO) was cultured to an OD_{600} of approximately 1.0. The culture was harvested by centrifugation at 5000*g* for 5 min. Ten milliliters of the cell suspension (approximately 10^8 cells) was used for protein extraction as described by von der Haar.[41]

HeLa cells were cultured in Dulbecco's Modified Eagle Medium, supplemented with 10% fetal bovine serum (Gibco) at 37 °C and a 5% CO_2 environment. Five $\times 10^6$HeLa cells were lysed on ice by three 30 s cycles of sonication in 1 mL of RIPA buffer (MiSonix s1394 probe, amplitude -25) with two 30 s intervals. Proteins were acetone precipitated (80% acetone for 2 h at −20, followed by two 80% acetone washes).

Precipitated proteins from HeLa and *S. cerevisiae* were resuspended in 0.1% Rapigest and 100 mM HEPES (pH 8.5). As reported previously,[26] we found that using 50 mM TEAB for TMT labeling introduces significant contamination (m/z 317.28, 391.25, Supplementary Figure 1, Supporting Information). The proteins were reduced by addition of 5 mM DTT for 30 min, alkylated with 10 mM iodoacetamide for 1 h in darkness, and digested by trypsin overnight at 37 °C at 1:20 ratio of protease to protein. Trypsin was added twice at a 1:40 ratio once when digestion was initiated and once again 3 h later. Rapigest was removed by addition of TFA to 1% and centrifugation at 16000*g* for 30 min. Digested peptides were submitted for amino acid analysis (PNAC Facility, Department of Biochemistry, University of Cambridge) to estimate absolute quantities of peptide digests. The pH of the solution was adjusted to 8.5 with 1 M NaOH, and peptides were diluted to 1 mg/mL. TMT 6-plex tags were resuspended in 50 μL of acetonitrile. A total of 25 μL of tag was added per 50 μg of peptides as shown in Table 1. Peptides were labeled for 2 h at room temperature and at 4 °C overnight, after which they were acidified with 5% TFA to prevent further labeling. Samples containing *S. cerevisiae* and HeLa peptides were pooled separately diluted to 0.2 μg/μL and stored at −80 °C.

LC−TWIMS-MS Configuration

For G2S experiments the peptides were separated on a nanoAquity UPLC system (Waters) and analyzed by a Synapt G2S TWIMS-MS hybrid instrument (Waters). Formic acid (0.1%, v/v) in water was used as buffer A, and 0.1% formic acid (v/v) in acetonitrile was used as buffer B. The samples were first trapped on a Symmetry C18 5 μm, 180 μM × 20 mm precolumn (Waters) and desalted at 10 μL/min flow for 6 min with 100% A, after which they were separated with a 90 min 7−35% B gradient on a T3 1.8 μM, 75 μm × 250 mm (Waters) column at a flow-rate of 300 nL/min. After separation, the column was washed with 80% buffer B for 5 min and re-equilibrated with 3% buffer B for 15 min. The column temperature was maintained at 30 °C. For lock-mass correction, 100 fmol/μL [Glu1]-fibrinopeptide B (Glu-Fib) was infused at 500 nL/min as a reference compound and recorded for 1 s every 30 s. Data for both MS1 and MS2 scans were acquired in profile mode. MS1 scan of 300−200 m/z was performed for 500 ms, followed by fragmentation (MS2) of the three most intense precursor ions for 500 ms. A dynamic exclusion window of ±100 mDa m/z was created for 60 s around ions that were sampled. Three sets of TWIMS were tested for G2S in this investigation, as summarized in Supplementary Table 1 (see Results and Discussion for explanation). A wide quadrupole transmission window was set at LM 4.7 and HM 15.7 (which corresponds to ion transmission window of 2 m/z before and 2 m/z units after the target m/z). A narrow quadrupole transmission window was set at 12.7 LM, HM 15.5 (which corresponds to an ion transmission window of 1 m/z before and 0.5 m/z units after the target m/z).

For experiments on G2Si platform, the LC method was as described above, but the gradient length was increased to 180 min to maximize the number of fragmentation events. Data for both MS1 and MS2 scans were acquired in profile mode. MS1 scan of 330−1600 m/z was performed for 200 ms, followed by fragmentation (MS2) of up to five most intense precursor ions for 500 ms, if their intensity rose above 20000. A dynamic exclusion window of ±500 mDa m/z was created for 60 s around ions that were sampled. A wide quadrupole transmission window was set at LM 4.7 and HM 16 (which corresponds to an ion transmission window of 2 m/z before and 2 m/z units after the target m/z). A narrow quadrupole transmission window was set at 15 LM, HM 16 (which corresponds to ion transmission window of 1 m/z before and 1 m/z units after the target m/z).

Data Analysis

The raw data files involving TWIMS reflect the acquisition method. Each mobility experiment (corresponding to survey scan or MS2 scan in conventional DDA when TWIMS is not enabled) is referred to as "block" and is composed of 200 TOF scans. The ion mobility profile is the ion intensity distribution across these 200 TOF scans. Each block in the mobility experiment was extracted individually by Waters proprietary algorithm ("CompressedDataCluster") in text format. It was then converted to mgf format. Tandem mass tag isotopic impurity correction and quantification of reporter ions was performed in the R MSnbase package.[42] All other analysis procedures were performed in R.[43] m/z targeted for fragmentation and retention time of MS2 blocks was extracted using SeeMS program from proteoWizard 3.0.4778 package.[44]

Deconvolution of precursor origin for G2S experiments is outlined in Supporting Information. For G2Si experiments mgfs for mascot search were created in ProteinLynx Global SERVER (PLGS) 3.01.[45] Mgfs were searched with Mascot 2.3.02 against combined *S. cerevisiae* and human database extracted from Uniprot (reference proteomes, canonical

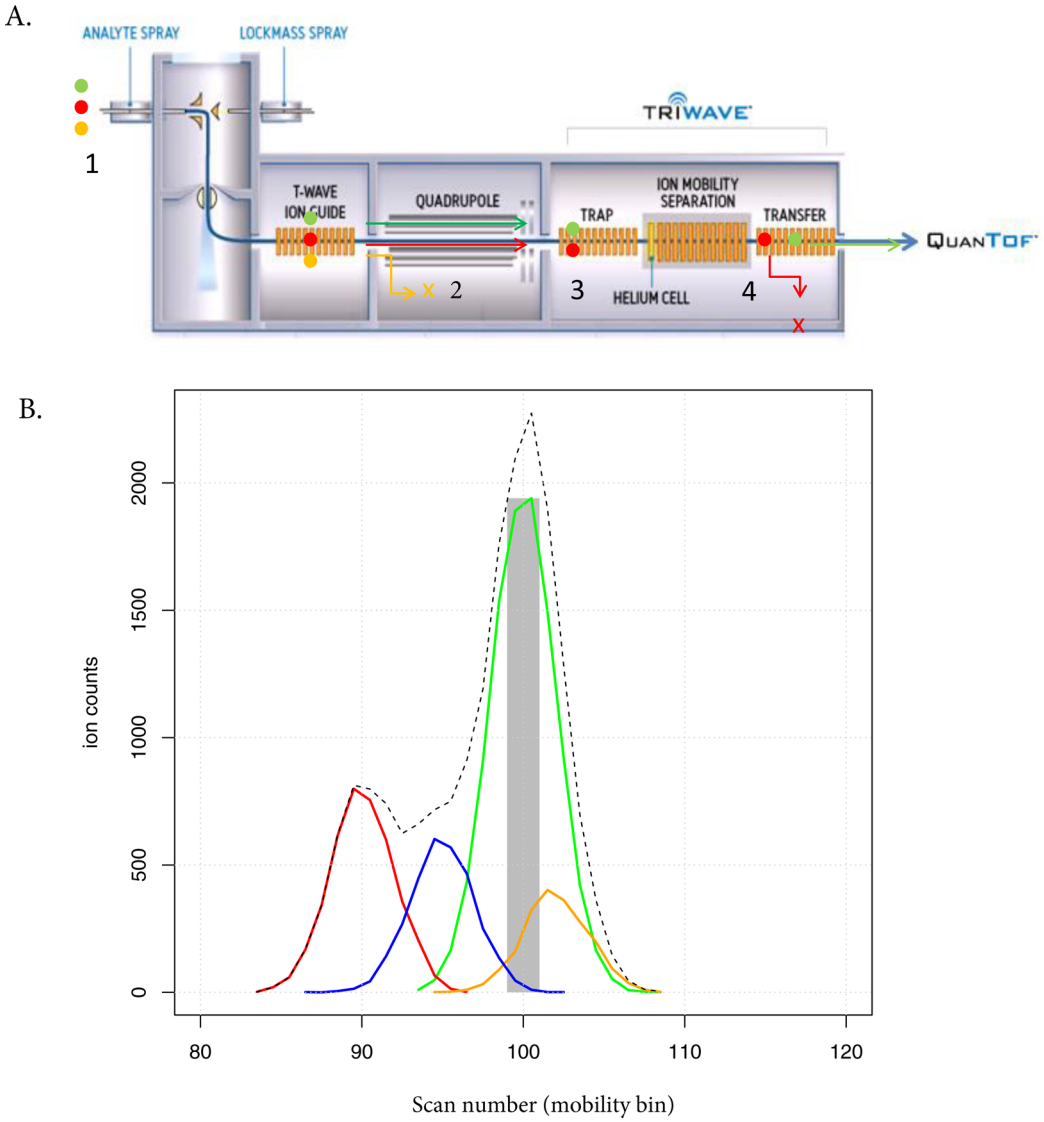

Figure 1. Peptide selection by quadrupole (m/z) and TWIMS (drift time). (A) instrument illustration. Stage 1: three peptides (yellow, green, and red) coelute from LC and enter the instrument. Green peptide is targeted for fragmentation. Stage 2: green peptide is isolated by quadrupole. While yellow peptide is discarded red peptide (having a similar m/z to green peptide) is coselected. Stage 3: the peptides are trapped in the TRAP part of TriWave awaiting their turn to be subjected to TWIMS. Stage 4: the ions are separated by TWIMS. Green and red ions are now fragmented in different mobility bins, and hence their spectra are recorded separately. (B) TWIMS purification example. Continuous lines represent intensities for four peptides (red, blue, green, yellow) in the 200 spectra (only bins 80−120 shown) comprising the mobility experiments, dotted line represents TIC (combined intensity for the four peptides). Green line corresponds to target (most intense) peptide, red, blue, and yellow lines correspond to contaminant ions. Bin number 100 has the highest TIC. Its selection is referred to as "TWIMS purification". Notably as expected it contains the target ion apex.

versions) with 10 ppm mass tolerance for precursors and 0.05 Da tolerance for fragment ions. Carbamidomethyl (C), TMT6plex (K), and TMT6plex (N-term) were selected as fixed modifications and Oxidation (M) and TMT6plex (Y) were selected as variable modifications. The data were also searched against decoy database. Peptides with scores higher than 20 were considered reliably identified, which corresponded to FDR of around than 5%.

RESULTS AND DISCUSSION

In order to address the well documented problem of precursor coselection[11] we incorporated TWIMS in the LC−MS workflow on a Synapt instrument series, using a mixture of *S. cerevisiae* and HeLa proteomes as a standard.

A schematic of consecutive peptide isolation by LC, quadrupole mass filter, and TWIMS is shown in Figure 1A. Peptides of the target m/z are first eluted from the column and selected by quadrupole mass filtering, and they are then trapped in the TRAP section of the TriWave, prior to being subjected to IMS. Any contaminants coselected with the target peptide by quadrupole mass filtering are trapped as well. The target peptide and contaminants are then injected into the IMS section of TriWave and, if separated there, are subsequently fragmented independently (i.e., their fragments will be recorded in different MS scans of IMS experiment). It should then be possible to select the MS scans corresponding to the peptide of interest while ignoring all the other scans containing contaminants. This approach is used while separating isomeric (i.e., also isobaric) peptides that have the same amino acid

dx.doi.org/10.1021/pr500220g | J. Proteome Res. 2014, 13, 3360−3369

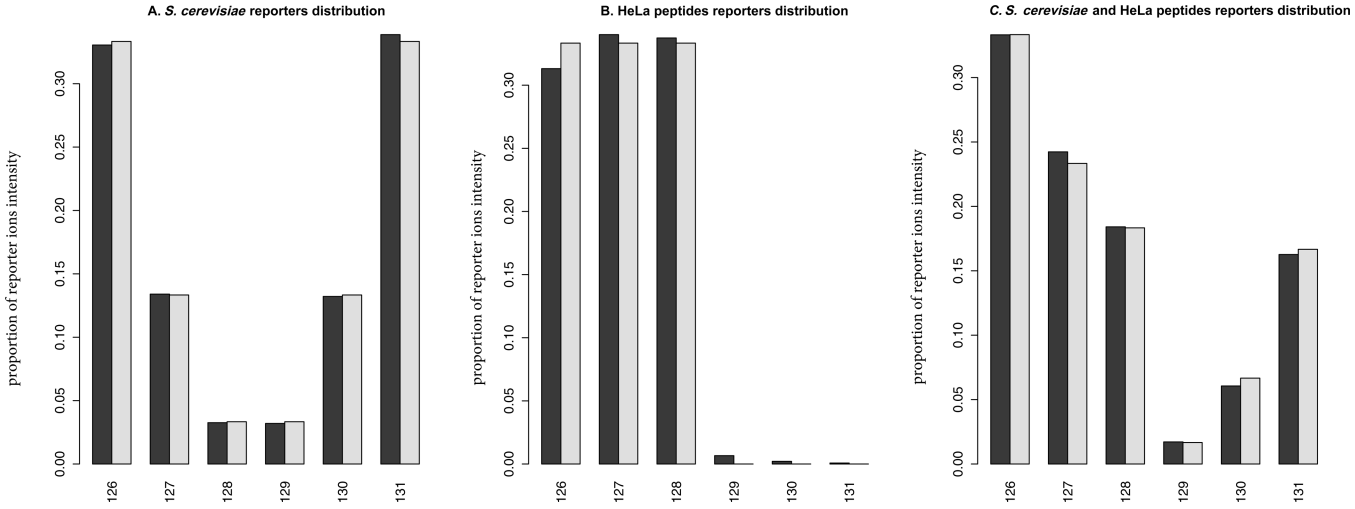

Figure 2. Expected (gray bars) and observed (black bars) distributions of reporters intensity in *S. cerevisiae* portion of the standard (A); HeLa portion of the standard (B); *S. cerevisiae* and HELA portions of the standard combined at 1:1 ratio.

composition but reversed sequences, which is a standard test of TWIMS performance.[38]

Standard Validation

The standard used in this study was prepared as described by Ting et al.[26] The expected TMT 6-plex reporter ion ratios for *S. cerevisiae* and HeLa peptides were 10:4:1:1:4:10 and 10:10:10:0:0:0 respectively. To validate these expected reporter ion ratios, *S. cerevisiae* and HeLa peptides were first analyzed independently in MS^E and then combined at a ratio of 1:1 and analyzed together. MS^E is a data-independent acquisition method whereby all coeluting precursors are first analyzed intact (MS or low energy scan) and are then cofragmented together (high energy scan). The data from the high-energy function (equivalent to MS/MS and liberation of isobaric tag reporter ions in a DDA experiment) were then combined, centroided, and corrected for TMT reagent isotopic impurities. The recorded and expected reporter ion ratios were found to be highly consistent (Figure 2). This demonstrates successful labeling, accurate pipetting while mixing of peptides labeled with different tags and accurate protein quantitation for *S. cerevisiae* and HeLa portions of the standard by amino acid analysis.

Effects of TWIMS Purification and Quadrupole Transmission Window on TMT Quantitative Accuracy

Increasing quadrupole resolution by narrowing the quadrupole transmission window is a simple and intuitive way to increase the purity of a peptide selected for fragmentation. If the quadrupole transmission window is extremely narrow, a peptide ion can be exclusively isolated for fragmentation and no reporter ion distortion will occur. Practically, current commercially available quadrupoles are low resolution mass filters, with top resolution at around 2000. Supplementary Figure 2, Supporting Information illustrates a representative spectrum of a peptide targeted for fragmentation. In a TOF survey scan with nominal resolution of 20000, many contaminant ions are visible near m/z of the target peak. These contaminants would be coselected with the target peptide for fragmentation by a default quadrupole transmission window of around 3−4 m/z on the Synapt instrument series. Supplementary Figure 3A, Supporting Information describes the settings that control quadrupole transmission window on Synapt instrument series, while Supplementary Figure 3B and Supplementary Methods, Supporting Information demonstrate a quick and simple method to relate these settings to transmission window shape by direct infusion.

Data-dependent acquisitions involving TWIMS are composed of alternating IMS experiments, recording drift times and m/z of precursors (survey scan in conventional DDA) and fragments generated from precursors isolated by the quadrupole (MS2 scan in conventional DDA). Each IMS experiment is composed of 200 TOF scans. The ion mobility profile of an ion is its intensity distribution across these 200 TOF scans. We reasoned that the TOF scan in a fragment IMS experiment that has the most intense reporter ions should also contain ions primarily originating from the precursor selected for fragmentation, since given that it is the most intense MS1 ion, it should also liberate the most intense reporters. Henceforth, we refer to TWIMS purification as selecting a single TOF scan (out of 200) having the highest intensity reporters in the fragment IMS experiment (see Figure 1B for explanation). To illustrate the reporter distributions if no TWIMS purification was performed, we combined the 200 TOF scans for each fragment mobility experiment, hence effectively eliminating IMS dimension from the recorded data. As a result every TWIMS-DDA acquisition provided two data sets: with TWIMS purification (only the highest intensity scan for every fragment mobility experiment selected) and without TWIMS purification (all 200 scans for each fragment mobility experiment combined). This allowed us to estimate reporter contamination with and without TWIMS purification under an identical instrumental setup, which is important, since as demonstrated previously enabling TWIMS can affect ion transmission.[55]

Using the mixed proteomes standard we have performed DDA-mobility experiments on G2Si platform with wide (4 Da) and narrow (2 Da) quadruple transmission window and then applied TWIMS purification postacquisition to benchmark system performance with four different precursor isolation methods: wide quadrupole, narrow quadrupole, wide quadrupole with TWIMS purification, narrow quadrupole with TWIMS purification.

Given that only *S. cerevisiae* peptides were labeled with 129−131 TMT tags, reporter contamination for HeLa peptides was

dx.doi.org/10.1021/pr500220g | J. Proteome Res. 2014, 13, 3360−3369

computed as shown by eq 1 and contamination of *S. cerevesiae* reporters as shown in eq 2.

$$\text{HeLa cont} = [(\text{int } 129 + \text{int } 130 + \text{int } 131) \times 2] / [\text{int } 126 + \text{int } 126 + \text{int } 127 + \text{int } 128 + \text{int } 129 + \text{int } 130 + \text{int } 131] \quad (1)$$

$$\textit{S. cerevisiae} \text{ cont} = 1 - [(\text{int } 129 + \text{int } 130 + \text{int } 131) \times 2] / [\text{int } 126 + \text{int } 126 + \text{int } 127 + \text{int } 128 + \text{int } 129 + \text{int } 130 + \text{int } 131] \quad (2)$$

where int126, int126, int127, int128, int129, int130, and int131 are intensities of reporter ions.

The results of investigation are presented in Supplementary Table 2 and Figure 3, Supporting Information. With a wide (4 *m/z*) quadrupole transmission window, the reporters are on average significantly contaminated (25% for HeLa and 24% contamination for *S. cerevisiae* peptides). Narrowing the quadrupole transmission window decreases contamination by around 10%, while performing TWIMS purification decreases precursor contamination by approximately 8%. Finally, application of TWIMS together with a narrow quadrupole transmission window results in cumulative gains in quantitative performance, leading to further decrease in contamination to around 9% for HeLa peptides and 6% of *S. cerevisiae* peptides. Though combination of narrow quadrupole selection and TWIMS purification did not completely alleviate the problem of coselection, it increased the median 126/128 reporter intensity ratio from 3.39 to 8.45 for *S. cerevisiae* peptides (10 being expected ratio).

It has previously been reported that FAIMS purification could be used to decrease MS2 noise and hence to increase peptide identification rate, especially in the case of lower abundant peptides.[46−50] The effect was mostly attributed to reducing noise coming from singly charged ion species. Given that TWIMS is a higher resolution technique than FAIMS,[51] and that it has already been demonstrated to effectively remove singly charged contaminants[38] a similar effect is expected on G2Si platform.

Unfortunately the software used in this study for noise reduction, deisotoping, centroiding, and lock mass correction (PLGS v3.01) does not currently support processing of individual scans within fragment or precursor mobility experiments (in fact it works with the data where IMS dimension has been eliminated by combining all scans within each IMS experiment). Hence we could not perform separate database searches on TWIMS mobility purified and nonpurified spectra. However, we were able to estimate the relative decrease in abundance for b- and y- sequence ions, as well as noise peaks not attributed to fragmentation products of the target peptide upon TWIMS precursor purification for all identified peptides. We estimate that 37.9% of b- and y- ion intensity and 13.3% noise intensity are on average present in the most intense (TWIMS purified) mobility bin. This corresponds to S/N ratio increase of over 2.84-fold at the cost of 62% sensitivity. Remarkably, almost 84% of contaminant ions are removed entirely (as opposed to 13% of b- and y-ions), giving the spectra an overall cleaner view (Figure 4 gives an example peptide and Supplementary Figure 4, Supporting Information for 10 peptides chosen at random).

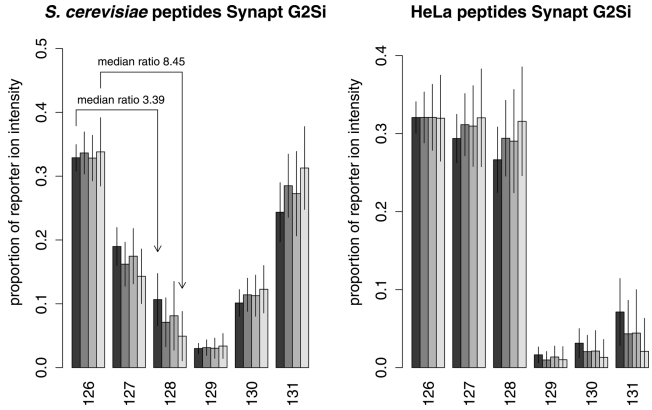

Figure 3. Distributions of reporter ion intensities for G2Si data normalized to the sum of 1 (for around 1200 and 1200 HELA peptides). Bars heights represent averages and error bars represent standard deviations. Each barplot contains four sets of bars which represent the following precursor purification methods (from left to right or from dark gray to light gray): (1) wide quadrupole transmission; (2) narrow quadrupole transmission; (3) wide quadrupole transmission with TWIMS purification; 4) narrow quadrupole transmission with TWIMS purification. The expected distributions of reporter intensities are 0.333:0.133:0.033:0.033:0.133:0.333 for *S. cerevisiae* and 0.333:0.333:0.333:0.000:0.000:0.000 for HeLa peptides. It is noteworthy that narrowing quadrupole transmission window and TWIMS purification results in cumulative gain in quantitative performance, resulting in 126−128 median ratio of 8.45.

Effect of TMT Labeling on Drift Time and *m/z*

The extent to which adding a new dimension of peptide separation increases the peak capacity of fractionation is dependent on the orthogonality of the fractionation methods.[40] Orthogonality is defined as lack of correlation between the position of an analyte peak in different dimensions.[39] Increased correlation indicates a decrease in methods orthogonality. Drift time and *m/z* of unlabeled peptides are known to correlate.[38] If TMT labeling changes the degree of this correlation it would also change how much TWIMS adds to LC−MS peak capacity.

Figure 5a,b demonstrates the plots of *m/z* against drift time for the 30000 most intense peptides for samples labeled and not labeled with TMT 6-plex respectively, stratified by precursor ion charge state. Several observations are noteworthy: there are more peptides at high *m/z* in the sample not labeled with TMT 6-plex; peptides with different charge states tend to overlap more in labeled samples; overall the correlation between *m/z* and drift time is higher for TMT labeled samples. The smaller *m/z* for labeled peptides (median of 577.6 ± 162 SD, compared to 633.39 ± 192SD for labeled peptides) despite the addition at least one 229 *m/z* TMT moiety to each tryptic peptide can be explained by charge enhancement. TMT derivatization is known to introduce numerous additional potential sites of protonation to the peptide.[52] Consequently, a higher proportion of TMT 6-plex labeled peptides will ionize with charge states of 3+ and higher than for unlabeled peptides, resulting in a lower median *m/z* despite an increase in mass (Supplementary Figure 5, Supporting Information). More interesting is that 2, 3, and 4+ ion clusters, which are almost completely resolved in drift time for unlabeled peptides, tend to overlap much more after TMT 6-plex derivatization (Figure 5c,d).

The overall effects described above result in less effective use of *m/z* and drift time space by the labeled compared to

dx.doi.org/10.1021/pr500220g | J. Proteome Res. 2014, 13, 3360−3369

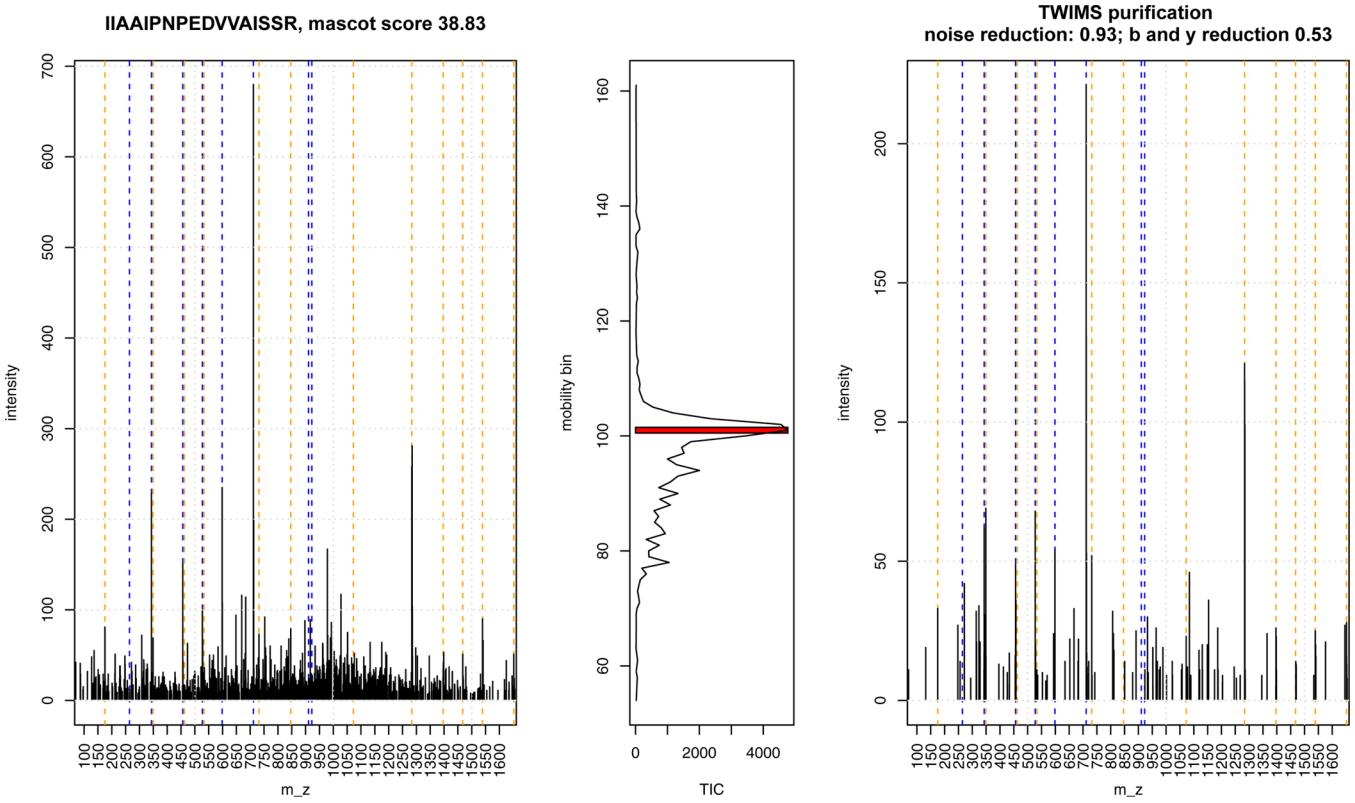

Figure 4. Illustration of b- (blue lines) and y- (yellow lines) ions purification. (Left) spectrum without TWIMS purification (i.e., all 200 spectra representing the mobility experiment are combined). (Middle) TIC in the 200 TOF spectra comprising the mobility experiment. Shown in red is the spectrum with the highest TIC (spectrum 99). (Right) Spectrum 99 (TWIMS purified spectrum) for IIAAIPNPEDVVAISSR peptide.

unlabeled peptides. In order to maximize the TWIMS resolution for isobaric mass tag labeled peptides analysis, we experimented with the pressure and wave velocity in the IMS section of the TriWave (as was suggested by the manufacturer) on G2S platform. Higher pressure in the IMS section of the TriWave is known to increase IMS resolution[53,54] but is also known to decrease the sensitivity of IMS due to scattering of ions during their entry into IMS zone.[38,55] Increasing the wave velocity from 700 m/s to 1100 m/s could potentially provide an increase in resolution, since at higher velocities the IMS peaks tend to be further apart. This would visually result in peptides occupying a larger proportion of IMS-MS space than shown on the plot (Figure 5A). However, at higher wave velocities the peaks themselves broaden, which decreases the IMS resolution. Broader IMS distributions lead to a less intense apical scan and, given that TWIMS purification is basically selecting this scan, the decrease in reporter intensity is thus anticipated (Supplementary Figure 6, Supporting Information).

Six DDA-mobility acquisitions were carried out using narrow and wide quadrupole transmission windows and three different settings for TWIMS (Supplementary Table 1, Supporting Information): (1) default settings ("700_m/s_low_pressure"); (2) increased wave velocity ("1100_m/s_low_pressure"); (3) increased flow of gas and hence increased pressure in IMS part of TriWave ("700_m/s_high_pressure").

Interestingly we did not observe a significant increase in quantitation accuracy with either higher pressure or increased wave velocity (Supplementary Table 3, Supplementary Figure 7, Supporting Information). Both increasing the pressure in IMS zone ("700_m/s_high_pressure") or wave velocity ("1100_m/s_low_pressure"), however, resulted in an approximately 2-fold decrease in reporter ion intensity compared to standard settings ("700_m/s_high_pressure") .

CONCLUSIONS

Ion mobility separation is increasingly utilized in conjunction with mass spectrometry. The recent release of IMS-MS by all major LC−MS vendors suggests that the role of IMS would further increase in proteomics workflows. It is however important to realize that IMS is still a low resolution technique compared to state-of-the art LC and MS systems. While it is capable of resolving ion species of significantly different chemical composition or different charge states, it is challenging to completely separate ion species of similar chemical composition and the same charge. This is evident from our data: although TWIMS successfully separates chemical contaminants from the target peptides, it is however less effective in separating contaminating peptides from target peptides of the same charge state. This results in remarkable improvements in the S/N ratio for b- and y-ion series necessary for peptide identification (up to 2.84, meaning contamination is reduced by around 90%) but only a modest improvement in isobaric mass tagging quantitative accuracy (contamination is reduced by one-third). Our data also demonstrate that labeling with isobaric mass tags causes peptides to have more uniform drift time distribution. This can partially be explained by charge state enhancement, a known problem associated with peptide derivatization with isobaric mass tags, but also results from peptides with different charge states having more similar mobilities than unlabeled peptides. Our efforts to optimize TWIMS resolution for labeled peptides by either increasing wave height or pressure in IMS cell did not result in a

dx.doi.org/10.1021/pr500220g | J. Proteome Res. 2014, 13, 3360−3369

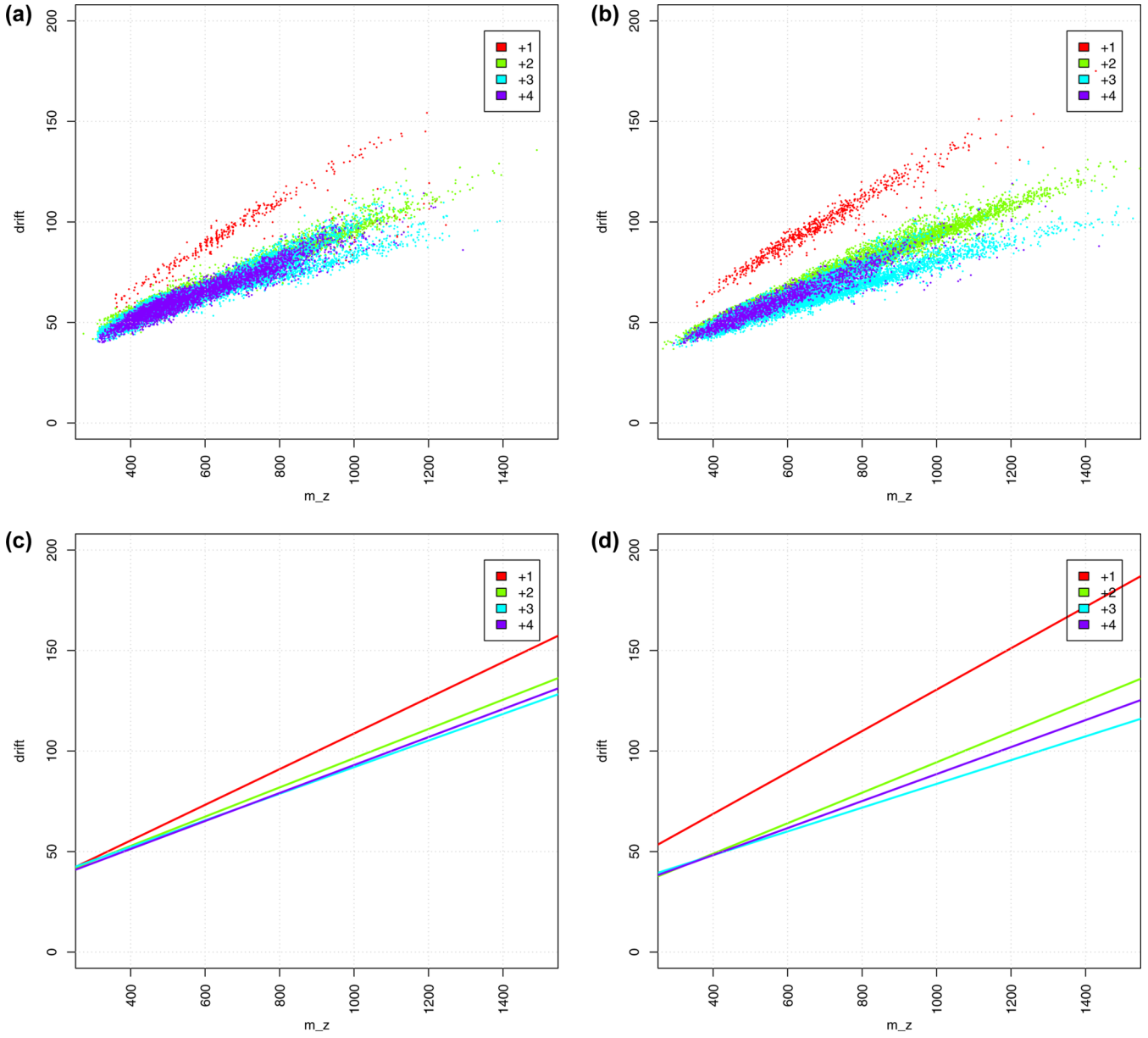

Figure 5. *m*/*z* and drift times in samples labeled (a and c) and not labeled (b and d) with TMT. (a and b) individual peptides, (c and d) *m*/*z* and drift time correlation trend lines. The *m*/*z* vs drift time trend lines for different charge states are much closer for TMT labeled peptides than for underivatized peptides.

significant gain of quantitation accuracy, suggesting that TWIMS is performing close to its maximum resolution at the standard settings suggested by manufacturer (Supplementary Table 1, Supporting Information). Despite all these challenges, a combination of narrow quadrupole transmission window, TWIMS purification, and 3 h gradient resulted in reporter ratios close to expected. For example the median 126/128 reporter intensity ratio shifted from 3.39 to 8.45 for *S. cerevisiae* peptides (10 being expected ratio).

The quantitative performance achieved in this study is interesting in the light of new acquisition methods (MS3 and QuantMode) aimed at restoring TMT quantitation accuracy reported recently for LTQ-Orbitrap platforms (though adequate comparison would require the same batch of standard to be analyzed by these methods with the same LC separation). While MS3 method reported by Ting and co-workers essentially restored quantitation accuracy, QuantMode described by Wenger and colleagues shifted the median ratio from 4.4:1 to 8.5:1(10 being expected), which is remarkably similar to the results of this study. A potential benefit of TWIMS purification among these three methods is that it also increases the quality of MS2 spectra for b- and y-ion series, while application of both MS3 and QuantMode methods results in a decrease of the number of peptide identifications, due to increased duty cycle.

It is also important to note that the standard used in this study (a mixture of two proteomes) has an abnormally high complexity, and incorporating another dimension of peptide separation by LC (SCX or high pH RP), as is standard for isobaric mass tagging workflows, should bring additional improvements in quantitative accuracy.

Future efforts in IMS instrument design will focus on improvement of this technique resolution. It is also expected that increased IMS resolution will make exchange of sensitivity

dx.doi.org/10.1021/pr500220g | *J. Proteome Res.* 2014, 13, 3360−3369

to additional peak capacity upon IMS application to LC−MS more favorable. The new developments of cyclical drift tubes look very promising in this respect already reporting resolutions in excess of 1000 (ref 56).

■ ASSOCIATED CONTENT

Supporting Information

Supplemental figures, tables and methods description. This material is available free of charge via the Internet at http://pubs.acs.org.

■ AUTHOR INFORMATION

Corresponding Author

*E-mail: k.s.lilley@bioc.cam.ac.uk. Tel: +441223760255. Fax: +441223760241.

Notes

The authors declare no competing financial interest.
The mass spectrometry proteomics data have been deposited to the ProteomeXchange Consortium[57] via the PRIDE partner repository with the dataset identifier PXD001047.

■ ACKNOWLEDGMENTS

The authors acknowledge Kevin Giles, Nick Tomczyk, Julien Bourquin, Keith Richardson, and Hans Vissers of Waters for their prompt and efficient help with MS software and hardware. We also thank Michael Deery for his advice and assistance with the mass spectrometry and Laurent Gatto for his advice on R programming. P.V.S. was funded through a studentship from The Darwin Trust of Edinburgh.

■ REFERENCES

(1) Michalski, A.; Damoc, E.; Hauschild, J.-P.; Lange, O.; Wieghaus, A.; Makarov, A.; Nagaraj, N.; Cox, J.; Mann, M.; Horning, S. Mass spectrometry-based proteomics using Q Exactive, a high-performance benchtop quadrupole Orbitrap mass spectrometer. *Mol. Cell Proteomics* **2011**, *10*, M111.011015.

(2) Webb, K. J.; Xu, T.; Park, S. K.; Yates, J. R., 3rd Modified MuDPIT separation identified 4488 proteins in a system-wide analysis of quiescence in yeast. *J. Proteome Res.* **2013**, *12*, 2177−2184.

(3) Hebert, A. S.; Richards, A. L.; Bailey, D. J.; Ulbrich, A.; Coughlin, E. E.; Westphall, M. S.; Coon, J. J. The one hour yeast proteome. *Mol. Cell Proteomics* **2014**, *13*, 339−347.

(4) Yao, X.; Freas, A.; Ramirez, J.; Demirev, P. A.; Fenselau, C. Proteolytic 18O labeling for comparative proteomics: model studies with two serotypes of adenovirus. *Anal. Chem.* **2001**, *73*, 2836−2842.

(5) Jiang, H.; English, A. M. Quantitative analysis of the yeast proteome by incorporation of isotopically labeled leucine. *J. Proteome Res.* **2002**, *1*, 345−350.

(6) Ong, S.-E.; Kratchmarova, I.; Mann, M. Properties of 13C-substituted arginine in stable isotope labeling by amino acids in cell culture (SILAC). *J. Proteome Res.* **2003**, *2*, 173−181.

(7) Oda, Y.; Huang, K.; Cross, F. R.; Cowburn, D.; Chait, B. T. Accurate quantitation of protein expression and site-specific phosphorylation. *Proc. Natl. Acad. Sci. U.S.A.* **1999**, *96*, 6591−6596.

(8) Hsu, J.-L.; Huang, S.-Y.; Chow, N.-H.; Chen, S.-H. Stable-isotope dimethyl labeling for quantitative proteomics. *Anal. Chem.* **2003**, *75*, 6843−6852.

(9) Thompson, A.; Schäfer, J.; Kuhn, K.; Kienle, S.; Schwarz, J.; Schmidt, G.; Neumann, T.; Johnstone, R.; Mohammed, A. K. A.; Hamon, C. Tandem mass tags: a novel quantification strategy for comparative analysis of complex protein mixtures by MS/MS. *Anal. Chem.* **2003**, *75*, 1895−1904.

(10) Hebert, A. S.; Merrill, A. E.; Bailey, D. J.; Still, A. J.; Westphall, M. S.; Strieter, E. R.; Pagliarini, D. J.; Coon, J. J. Neutron-encoded mass signatures for multiplexed proteome quantification. *Nat. Methods* **2013**, *10*, 332−334.

(11) Schulze, W. X.; Usadel, B. Quantitation in mass-spectrometry-based proteomics. *Annu. Rev. Plant Biol.* **2010**, *61*, 491−516.

(12) Wang, J.; Pérez-Santiago, J.; Katz, J. E.; Mallick, P.; Bandeira, N. Peptide Identification from Mixture Tandem Mass Spectra. *Mol. Cell Proteomics* **2010**, *9*, 1476−1485.

(13) Geromanos, S. J.; Hughes, C.; Golick, D.; Ciavarini, S.; Gorenstein, M. V.; Richardson, K.; Hoyes, J. B.; Vissers, J. P. C.; Langridge, J. I. Simulating and validating proteomics data and search results. *Proteomics* **2011**, *11*, 1189−1211.

(14) Luethy, R.; Kessner, D. E.; Katz, J. E.; MacLean, B.; Grothe, R.; Kani, K.; Faça, V.; Pitteri, S.; Hanash, S.; Agus, D. B.; Mallick, P. Precursor-Ion Mass Re-Estimation Improves Peptide Identification on Hybrid Instruments. *J. Proteome Res.* **2008**, *7*, 4031−4039.

(15) Houel, S.; Abernathy, R.; Renganathan, K.; Meyer-Arendt, K.; Ahn, N. G.; Old, W. M. Quantifying the impact of chimera MS/MS spectra on peptide identification in large-scale proteomics studies. *J. Proteome Res.* **2010**, *9*, 4152−4160.

(16) Michalski, A.; Cox, J.; Mann, M. More than 100,000 detectable peptide species elute in single shotgun proteomics runs but the majority is inaccessible to data-dependent LC-MS/MS. *J. Proteome Res.* **2011**, *10*, 1785−1793.

(17) Kalli, A.; Smith, G. T.; Sweredoski, M. J.; Hess, S. Evaluation and Optimization of Mass Spectrometric Settings during Data-dependent Acquisition Mode: Focus on LTQ-Orbitrap Mass Analyzers. *J. Proteome Res.* **2013**, *12*, 3071−3086.

(18) Wong, C. C. L.; Cociorva, D.; Venable, J. D.; Xu, T.; Yates, J. R., 3rd Comparison of different signal thresholds on data dependent sampling in Orbitrap and LTQ mass spectrometry for the identification of peptides and proteins in complex mixtures. *J. Am. Soc. Mass Spectrom.* **2009**, *20*, 1405−1414.

(19) Bantscheff, M.; Boesche, M.; Eberhard, D.; Matthieson, T.; Sweetman, G.; Kuster, B. Robust and sensitive iTRAQ quantification on an LTQ Orbitrap mass spectrometer. *Mol. Cell Proteomics* **2008**, *7*, 1702−1713.

(20) Ow, S. Y.; Salim, M.; Noirel, J.; Evans, C.; Wright, P. C. Minimising iTRAQ ratio compression through understanding LC-MS elution dependence and high-resolution HILIC fractionation. *Proteomics* **2011**, *11*, 2341−2346.

(21) Karp, N. A.; Huber, W.; Sadowski, P. G.; Charles, P. D.; Hester, S. V.; Lilley, K. S. Addressing accuracy and precision issues in iTRAQ quantitation. *Mol. Cell Proteomics* **2010**, *9*, 1885−1897.

(22) Mahoney, D. W.; Therneau, T. M.; Heppelmann, C. J.; Higgins, L.; Benson, L. M.; Zenka, R. M.; Jagtap, P.; Nelsestuen, G. L.; Bergen, H. R.; Oberg, A. L. Relative quantification: characterization of bias, variability and fold changes in mass spectrometry data from iTRAQ-labeled peptides. *J. Proteome Res.* **2011**, *10*, 4325−4333.

(23) Breitwieser, F. P.; Müller, A.; Dayon, L.; Köcher, T.; Hainard, A.; Pichler, P.; Schmidt-Erfurth, U.; Superti-Furga, G.; Sanchez, J.-C.; Mechtler, K.; Bennett, K. L.; Colinge, J. General Statistical Modeling of Data from Protein Relative Expression Isobaric Tags. *J. Proteome Res.* **2011**, *10*, 2758−2766.

(24) Evans, C.; Noirel, J.; Ow, S. Y.; Salim, M.; Pereira-Medrano, A. G.; Couto, N.; Pandhal, J.; Smith, D.; Pham, T. K.; Karunakaran, E.; Zou, X.; Biggs, C. A.; Wright, P. C. An insight into iTRAQ: where do we stand now? *Anal Bioanal Chem.* **2012**, *404*, 1011−1027.

(25) Christoforou, A. L.; Lilley, K. S. Isobaric tagging approaches in quantitative proteomics: the ups and downs. *Anal Bioanal Chem.* **2012**, *404*, 1029−1037.

(26) Ting, L.; Rad, R.; Gygi, S. P.; Haas, W. MS3 eliminates ratio distortion in isobaric multiplexed quantitative proteomics. *Nat. Methods* **2011**, *8*, 937−940.

(27) Ow, S. Y.; Salim, M.; Noirel, J.; Evans, C.; Rehman, I.; Wright, P. C. iTRAQ underestimation in simple and complex mixtures: "the good, the bad and the ugly. *J. Proteome Res.* **2009**, *8*, 5347−5355.

(28) Breitwieser, F. P.; Müller, A.; Dayon, L.; Köcher, T.; Hainard, A.; Pichler, P.; Schmidt-Erfurth, U.; Superti-Furga, G.; Sanchez, J.-C.; Mechtler, K.; Bennett, K. L.; Colinge, J. General Statistical Modeling of

Data from Protein Relative Expression Isobaric Tags. *J. Proteome Res.* **2011**, *10*, 2758−2766.
(29) Zhang, Y.; Askenazi, M.; Jiang, J.; Luckey, C. J.; Griffin, J. D.; Marto, J. A. A robust error model for iTRAQ quantification reveals divergent signaling between oncogenic FLT3 mutants in acute myeloid leukemia. *Mol. Cell Proteomics* **2010**, *9*, 780−790.
(30) Hundertmark, C.; Fischer, R.; Reinl, T.; May, S.; Klawonn, F.; Jänsch, L. MS-specific noise model reveals the potential of iTRAQ in quantitative proteomics. *Bioinformatics* **2009**, *25*, 1004−1011.
(31) Dayon, L.; Sonderegger, B.; Kussmann, M. Combination of gas-phase fractionation and MS^3 acquisition modes for relative protein quantification with isobaric tagging. *J. Proteome Res.* **2012**, *11*, 5081−5089.
(32) Haas W. Multiplexed Quantitative Proteomics Using Isobaric Labeling: Rationale, Status and Needs.
(33) Wenger, C. D.; Lee, M. V.; Hebert, A. S.; McAlister, G. C.; Phanstiel, D. H.; Westphall, M. S.; Coon, J. J. Gas-phase purification enables accurate, multiplexed proteome quantification with isobaric tagging. *Nat. Methods* **2011**, *8*, 933−935.
(34) Savitski, M. M.; Fischer, F.; Mathieson, T.; Sweetman, G.; Lang, M.; Bantscheff, M. Targeted data acquisition for improved reproducibility and robustness of proteomic mass spectrometry assays. *J. Am. Soc. Mass Spectrom.* **2010**, *21*, 1668−1679.
(35) Phillips, H. L.; Williamson, J. C.; van Elburg, K. A.; Snijders, A. P. L.; Wright, P. C.; Dickman, M. J. Shotgun proteome analysis utilising mixed mode (reversed phase-anion exchange chromatography) in conjunction with reversed phase liquid chromatography mass spectrometry analysis. *Proteomics* **2010**, *10*, 2950−2960.
(36) Lapthorn, C.; Pullen, F.; Chowdhry, B. Z. Ion mobility spectrometry-mass spectrometry (IMS-MS) of small molecules: separating and assigning structures to ions. *Mass Spectrom Rev.* **2013**, *32*, 43−71.
(37) Jiang, W.; Robinson, R. A. S. Ion Mobility-Mass Spectrometry. In *Encyclopedia of Analytical Chemistry*; John Wiley & Sons, Ltd: New York, 2006.
(38) Pringle, S. D.; Giles, K.; Wildgoose, J. L.; Williams, J. P.; Slade, S. E.; Thalassinos, K.; Bateman, R. H.; Bowers, M. T.; Scrivens, J. H. An investigation of the mobility separation of some peptide and protein ions using a new hybrid quadrupole/travelling wave IMS/oa-ToF instrument. *Int. J. Mass Spectrom.* **2007**, *261*, 1−12.
(39) Ruotolo, B. T.; Gillig, K. J.; Stone, E. G.; Russell, D. H. Peak capacity of ion mobility mass spectrometry: separation of peptides in helium buffer gas. *J. Chromatogr. B Analyt. Technol. Biomed. Life Sci.* **2002**, *782*, 385−392.
(40) Liu, Z.; Patterson, D. G.; Lee, M. L. Geometric Approach to Factor Analysis for the Estimation of Orthogonality and Practical Peak Capacity in Comprehensive Two-Dimensional Separations. *Anal. Chem.* **1995**, *67*, 3840−3845.
(41) Von der Haar, T. Optimized Protein Extraction for Quantitative Proteomics of Yeasts. *PLoS One* **2007**, *2*, e1078.
(42) Gatto, L.; Lilley, K. S. MSnbase-an R/Bioconductor package for isobaric tagged mass spectrometry data visualization, processing and quantitation. *Bioinformatics* **2012**, *28*, 288−289.
(43) R Core Team. *R: A Language and Environment for Statistical Computing*, 2013.
(44) Kessner, D.; Chambers, M.; Burke, R.; Agus, D.; Mallick, P. ProteoWizard: open source software for rapid proteomics tools development. *Bioinformatics* **2008**, *24*, 2534−2536.
(45) Li, G.-Z.; Vissers, J. P. C.; Silva, J. C.; Golick, D.; Gorenstein, M. V.; Geromanos, S. J. Database searching and accounting of multiplexed precursor and product ion spectra from the data independent analysis of simple and complex peptide mixtures. *Proteomics* **2009**, *9*, 1696−1719.
(46) Saba, J.; Bonneil, E.; Pomiès, C.; Eng, K.; Thibault, P. Enhanced sensitivity in proteomics experiments using FAIMS coupled with a hybrid linear ion trap/Orbitrap mass spectrometer. *J. Proteome Res.* **2009**, *8*, 3355−3366.
(47) Brown, L. J.; Toutoungi, D. E.; Devenport, N. A.; Reynolds, J. C.; Kaur-Atwal, G.; Boyle, P.; Creaser, C. S. Miniaturized ultra high field asymmetric waveform ion mobility spectrometry combined with mass spectrometry for peptide analysis. *Anal. Chem.* **2010**, *82*, 9827−9834.
(48) Bridon, G.; Bonneil, E.; Muratore-Schroeder, T.; Caron-Lizotte, O.; Thibault, P. Improvement of Phosphoproteome Analyses Using FAIMS and Decision Tree Fragmentation. Application to the Insulin Signaling Pathway in Drosophila melanogaster S2 Cells. *J. Proteome Res.* **2012**, *11*, 927−940.
(49) Swearingen, K. E.; Moritz, R. L. High-field asymmetric waveform ion mobility spectrometry for mass spectrometry-based proteomics. *Expert Rev. Proteomics* **2012**, *9*, 505−517.
(50) Creese, A. J.; Smart, J.; Cooper, H. J. Large-Scale Analysis of Peptide Sequence Variants: The Case for High-Field Asymmetric Waveform Ion Mobility Spectrometry. *Anal. Chem.* **2013**, *85*, 4836−4843.
(51) Lanucara, F.; Holman, S. W.; Gray, C. J.; Eyers, C. E. The power of ion mobility-mass spectrometry for structural characterization and the study of conformational dynamics. *Nat. Chem.* **2014**, *6*, 281−294.
(52) Thingholm, T. E.; Palmisano, G.; Kjeldsen, F.; Larsen, M. R. Undesirable charge-enhancement of isobaric tagged phosphopeptides leads to reduced identification efficiency. *J. Proteome Res.* **2010**, *9*, 4045−4052.
(53) Davis, E. J.; Grows, K. F.; Siems, W. F.; Hill, H. H., Jr Improved ion mobility resolving power with increased buffer gas pressure. *Anal. Chem.* **2012**, *84*, 4858−4865.
(54) Davis, E. J.; Dwivedi, P.; Tam, M.; Siems, W. F.; Hill, H. H. High-pressure ion mobility spectrometry. *Anal. Chem.* **2009**, *81*, 3270−3275.
(55) Shliaha, P. V.; Bond, N. J.; Gatto, L.; Lilley, K. S. Effects of traveling wave ion mobility separation on data independent acquisition in proteomics studies. *J. Proteome Res.* **2013**, *12*, 2323−2339.
(56) Glaskin, R. S.; Ewing, M. A.; Clemmer, D. E. Ion Trapping for Ion Mobility Spectrometry Measurements in a Cyclical Drift Tube. *Anal. Chem.* **2013**, *85*, 7003−7008.
(57) Vizcaíno, J. A.; Deutsch, E. W.; Wang, R.; Csordas, A.; Reisinger, F.; Ríos, D.; Dianes, J. A.; Sun, Z.; Farrah, T.; Bandeira, N.; Binz, P. A.; Xenarios, I.; Eisenacher, M.; Mayer, G.; Gatto, L.; Campos, A.; Chalkley, R. J.; Kraus, H. J.; Albar, J. P.; Martinez-Bartolomé, S.; Apweiler, R.; Omenn, G. S.; Martens, I.; Jones, A. R.; Hermjakob, H. 2014; ProteomeXchange provides globally co-ordinated proteomics data submission and dissemination. *Nature Biotechnol.* 30(3):223−226. PubMed PMID:24727771.